Role of conducting carbon in electrodes for electric double layer capacitors

Chris Dangler, Manisha Rane-Fondacaro *, Thamarai Selvi Devarajan, Seiichiro Higashiya, Jeremy Snyder, Pradeep Haldar

College of Nanoscale Science and Engineering, University at Albany, 257 Fuller Road, Albany, NY 12203, USA

ARTICLE INFO

ABSTRACT

Six electrodes with a varying amount (5, 10, and 15 wt.%) of conducting carbon nanotubes (CNT) and carbon nanofibers (CNF) were fabricated and their performance evaluated against a control sample that was devoid of any conducting material. The goal of this work was to determine the correlation between electrode conductivity and capacitance in 1 M tetraethyl ammonium tetrafluoroborate (TEABF$_4$) in propylene carbonate (PC) electrolyte. CNT electrodes exhibit the lowest electrical resistance, while CNF electrodes had the highest capacitance. The specific capacitance (120–140 F/g) increased monotonically up to 2.5 V. An inverse correlation between electrical resistance and capacitance was observed for various concentrations. The electrodes were characterized using CV, EIS, SEM, and BET analysis.

© 2010 Elsevier B.V. All rights reserved.

1. Introduction

Carbon based double layer capacitors typically exhibit a maximum energy density of ~4–5 Wh/kg [1], though insignificant in comparison with pseudocapacitors and advanced batteries [2], yet most favored for its reliability.

The specific capacitance of activated carbon varies between 100 and 220 F/g depending on the carbon and electrolyte used. For example, in aqueous electrolytes, the typical capacitance value is ~200 F/g, while in organics (propylene carbonate and acetonitrile) it is typically around 100 F/g [3].

Largeot et al. report an exceptionally high capacitance in carbon with a tailored porosity derived from carbide derived carbons (CDC) [4]. The unusually high conductivity ~140 S/cm (CDC) as compared with activated carbon (10–12 S/cm) arises from the absence of oxygen or hydrogen in its carbon network [5,6]. Coulomb's law dictates the direct proportionality of the electrostatic force to conductivity (and distance), and hence a higher capacitance. Moreover, the pore parameters (structure, size uniformity, and distribution) in these materials further facilitate high energy density [7], and high electrical conductivity is typical in pseudocapacitors [8].

This work investigates the role of conductivity enhancer additives such as CNT and CNF in the electrode matrix comprising of microporous activated carbon (YP-17 from Kuraray Chemicals; pore size range 1–1.265 nm and pore volume >55%). The main contribution to EDLC resistance arises from the electrolyte, followed by contact resistance between carbon particles. Aluminum current collector (Al-CC) is the third largest contributor to the EDLC resistance [13]. Here in this publication we report surface treatment of Al-CC with the goal to reduce its resistance.

2. Materials and methods

Six electrodes with a varying amount of conducting carbon materials were added to activated carbon with 5 wt.% Teflon binder, and the mixture was cast into 50 μm thin sheets. A benchmark seventh electrode comprised of activated carbon material and binder. The carbon sheet was attached to a pretreated Al-CC, EDLC cells constructed in a bag cell, and tested using (electrochemical impedance spectroscopy) EIS and (capacitance–voltage measurement) CV using a Potentiostat (PARSTAT 2273, Princeton Applied Research). The following sections provide a detailed description of the entire synthesis and testing procedure. Scanning Electron Microscope, (Model No. LEO-1550, Zeiss) was used for plane view and cross sectional imaging. BET (Brunauer, Emmett, and Teller) analysis was used to determine the pore size and electrode specific surface area (SSA) using NOVA 4200e (Quantachrome Instrument).

3. Results and discussion

3.1. Current collector

Appropriate chemical treatment [9–11] was provided to Al-CC prior to attachment of the activated carbon material for lowering the resistivity. As received aluminum foil (30 μm, 99.999% pure, All-Foils, Inc.) was used as the baseline. The first treatment (a) comprised of anodization treatment in 0.3 M oxalic acid for 40 min at 40 V and 1A. Surface oxide removal was performed in a bath of chromium oxide and phosphoric acid (at 60 °C/10 min), followed by DI (de-ionized) water rinse, and drying. Then the Al-CCs were transferred immediately to a glove box with a controlled atmosphere. The second treatment

* Corresponding author. Tel.: +1 518 956 7310; fax: +1 518 437 8687.
E-mail address: mrane@uamail.albany.edu (M. Rane-Fondacaro).
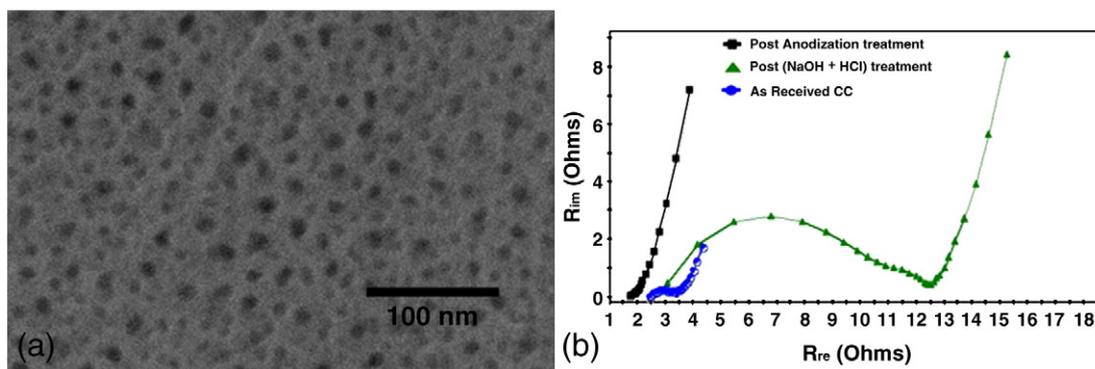
Fig. 1. (a) Al-CC post anodization treatment. (b) EIS of Al-CC: (o): as received Al foil (■): EIS of Al foil post anodization (▲): EIS of Al foil post (NaOH + HCl) treatment.

(b) comprised of degreasing in a sodium hydroxide (NaOH) solution for 5 min, followed by DI water rinse. Subsequently, the Al-CC was etched in a hydrochloric acid (HCl), solution for 30 s, followed by DI water rinse, and drying.

Fig. 1 shows the SEM images of Al foil post anodization (a) and (b) the resulting electrical impedance for anodized Al-CC, Al foil subject to alkali and acid treatment, and as received sample (reference). The anodized sample exhibits a uniform hexagonal pore structure, with an average pore size ~10 nm.

The as received sample (o) shows a resistive loop that is typical of a surface oxide layer. A drastic increase in resistance was observed in the sample treated with alkali and acid (▲), indicating the considerable thickness of aluminum oxide layer. Post-anodized foil (■) exhibits the lowest resistance, due to the dissolution of the surface aluminum oxide was in a hot phosphorous acid solution, and hence the semicircular loop was conspicuously absent. Optimization of time, voltage, and, current enabled a very low resistance of 0.43 Ω (not shown).

3.2. Freestanding carbon

Varying percentages (5%, 10%, and 15%) of multiwall CNT (PD30L15, NanoLab) and CNF (as grown-Pyrograf-1 grade, from Applied Sciences Inc.) were incorporated into six electrodes and their properties tested. All had 5.0 wt.% fibrillated Teflon 6 C (DuPont) as a binder, and the balance was activated carbon (YP-17, Kuraray Chemical Co. average particle size ~5 μm). The control sample was made of a pure activated carbon (AC and 5.0 wt.% binder) material.

The carbon mixture was heated at a 100 °C in nitrogen atmosphere, subsequently ground with a pestle. At 100 °C Teflon 6C softens becoming fibrous upon grinding. Upon repeated grinding of Teflon with activated carbon, the activated carbon material gets caught between the Teflon fibers thus forming a gooey lump. The activated carbon by itself was resistant to being ground. The bound carbon was then rolled out into sheets ~50 μm thick, and cut into a 4 cm^2 freestanding material.

Shown in Fig. 2 is a plane view and cross sectional electrode microstructure for varying CNT content. The CNT decoration on the top surface increases with the CNT content, while the CNT amount within the sample interior remains insignificant. The typical dimension of the CNT is ~1–5 μm length and a diameter~30 nm. CNTs typically clump together due to strong van der Waals force, hence difficult to incorporate within the cross section. On the other hand, as grown CNFs with a diameter~100–200 nm, length~3–10 μm, were easily dispersed within AC (~5 μm).

3.3. Electrode fabrication

The freestanding carbon tapes were attached to the Al foil using a conducting paste Electrodag (EB-012, Ladd Research Industries Inc.). The electrodes and polytetrafloroethylene (PTFE) separator
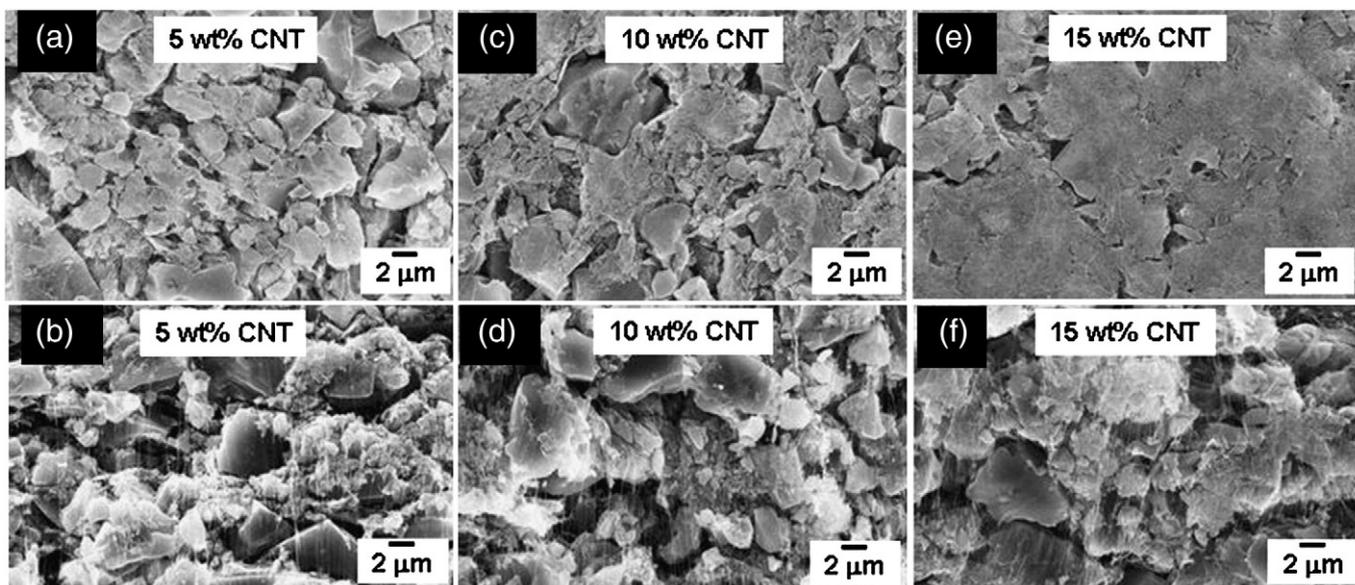
Fig. 2. SEM microstructure of CNT based electrodes (plane view, cross sectional view): (a, b) of 5 wt.% CNT. (c, d) 10 wt.% CNT and (e, f) 15 wt.% CNT.
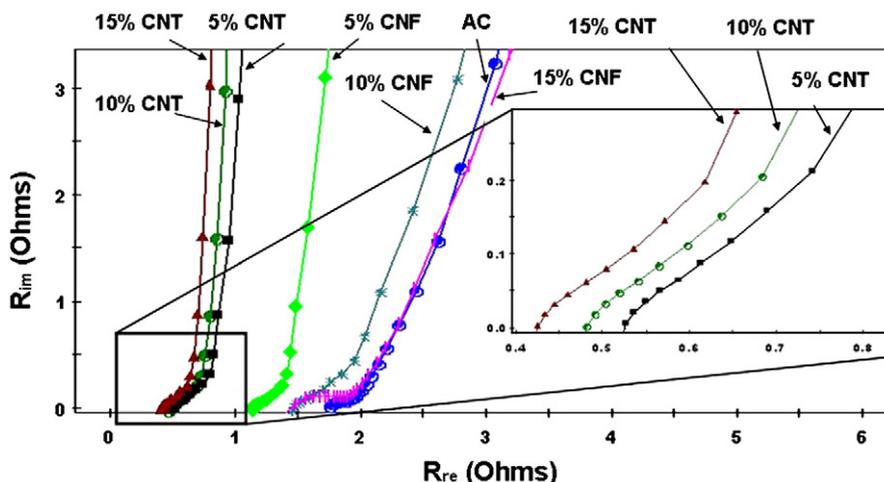
Fig. 3. EIS of all electrodes.

(34 μm, Excellerator Separator, Gore) were soaked in 1 M TEABF$_4$/PC (Honeywell) for 24 h. PTFE sheet was placed between two soaked electrodes, and together were sealed in a metalized bag with an addition of 0.3 mL electrolyte. Cells were immediately tested post fabrication.

3.4. Electrochemical testing

CV and EIS measurements were performed inside a glove box. Eight scans were run at 1.0 to 3.0 V range with a step size of 0.5 V, a scan rate of 5 mV/s for CV; and EIS scans were performed from 2 MHz to 10 MHz, to generate a Nyquist plot.

Fig. 3 shows the EIS curves for all EDLC samples post CV at 3 V. CNT based electrodes exhibit the lowest ESR, which reduced with increasing the CNT content. A wide ESR range is observed in CNF based electrodes that increased with the CNF concentration.

The semicircle was conspicuously absent in the high frequency range for the CNT electrodes, and in the 5 wt.% CNF electrode; while the 45° phase angle, a signature of Warburg impedance was observed in all the above electrodes indicating a double layer capacitance process [12].

Initiation of semicircle was observed in the 10 wt.% CNF electrode, and was well defined in 15 w.t% CNF and AC electrode. The AC electrode exhibits the highest ESR. The semicircle could possibly arise from electrolyte starvation effects leading to an increase in the contact resistance between adjacent carbon particles, or an increase in the electronic resistance between the current collectors − electrode material [12].

The measured BET values (mesoporous surface area) of CNT, CNF, and AC are 272 m^2/g, 61 m^2/g, and 1200 m^2/g respectively. The SSA of the electrodes was in the range of 1000–1200 m^2 /g, with no particular trend for samples.

Shown in Fig. 4 is the variation in the capacitance with the applied voltage. Capacitance increased linearly up to 2.5 V and then dropped at 3.0 V in all electrodes. The difference in the capacitance between various electrodes is insignificant at low voltages, but at 2.5 V and above, the CNF based electrodes show a higher capacitance than CNT and AC. The presence of a large amount of the CNF in the sample interior most probably opened up access pathways for the electrolyte. CNT incorporation on the other hand did not yield in any capacitance enhancement, as it did not go in the bulk of the electrode (Fig. 2), yet, led to the lowest ESR. It appears that the mere presence of CNT and CNF in electrodes are responsible for changing the electrode properties — most probably owing to interaction of numerous surface functionalities with the electrolyte.

4. Summary

In summary, electrodes with varying percentages (5 wt.%, 10 wt.% and 15 wt.%) of conductivity enhancers (CNT and CNF) and one control sample were fabricated with the aim to investigate the relation between capacitance and electrode conductivity. A 50 μm thick activated carbon tape was attached to a pretreated Al foil with a reduced resistance. The lowest ESR (0.4–0.55 Ω) and double layer capacitance behavior was observed in CNT (120–125 F/g) electrodes,
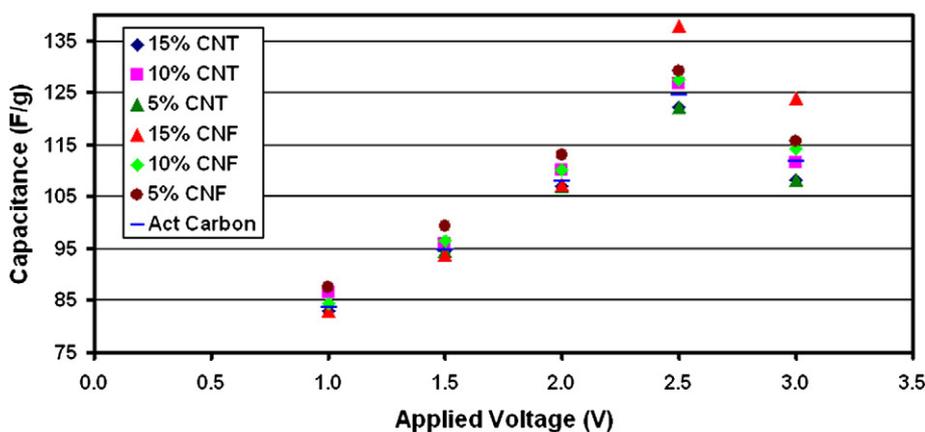
Fig. 4. Plot of capacitance variation with applied voltage for all electrodes.

while a higher capacitance was observed in CNF electrodes (125–140 F/g). Reduction in ESR was observed with increasing CNT content, while the opposite trend was noted in CNF electrodes. No direct correlation was established between electrode conductivity and ESR due to lack of dispersion of conductivity enhancers. Nevertheless, the presence of the CNF does lead to a better electrolyte penetration, and hence a higher capacitance, while CNT electrodes led to an enhanced electrode conductivity. We believe both of these to be artifacts of surface functionalities (on CNT and CNF) rather than conductivity effect. The BET surface area of all electrodes was in the range 1000–1200 m^2/g. A monotonic increase in the capacitance was observed with increasing voltage up to 2.5 V, and then it reduced at 3.0 V. The maximum capacitance value was observed at 2.5 V, in the range ~120–140 F/g, which is typically observed in organic electrolytes [3].

Acknowledgment

References

[1] Conway BE. Electrochemical Supercapacitors: Scientific Fundamentals and Technological Applications. Springer; 1999.
[2] Burke A. Electrochim Acta 2007;53:1083–91.
[3] Simon P, Burke A. The Electrochem. Soc. Interface; Spring 2008. p. 38–43.
[4] Largeot C, Portet C, Chmiola J, Taberna PL, Gogotsi Y, Simon P. J Am Chem Soc 2008;130:2730–1.
[5] Yushin G, Nikitin A, Gogotsi Y. In: Gogotsi Y, editor. Nanomaterials, Handbook. Boca Raton, FL: CRC Press; 2006. p. 237–80.
[6] Shukla AK, Sampath S, Vijayamohanan K. Curr Sci 2000;79:1656–61.
[7] Xing W, Qiao SZ, Ding RG, Li F, Lu GQ, Yan ZF, Cheng HM. Carbon 2006;44:216–24.
[8] Choi D, Kumta PN. J Electrochem Soc 2006;153(12):A2298–303.
[9] Portet C, Taberna PL, Simon P, Laberty-Robert C. Electrochim Acta 2004;49:905–12.
[10] Du Pasquier A, Plitz I, Menocal S, Amatucci G. J Power Sources 2003;115:171.
[11] Taberna PL, Simon P, Fauvarque JF. J Electrochim Soc 2003;150:292.
[12] Pell, Conway BE, Marincic N. J Electroanal Chem 2000;491(1):9–21.
[13] "Carbons for Electrochemical Energy Storage and Conversion Systems", Edited by: Francois Begum and Elzbieta Frackowiak, CRC Press, Taylor and Francis Group, 2010.